ESC European Society of Cardiology

European Heart Journal - Cardiovascular Imaging (2019) **0**, 1–12
doi:10.1093/ehjci/jez050

Imaging in patients with severe mitral annular calcification: insights from a multicentre experience using transatrial balloon-expandable valve replacement

**Fabien Praz[1†], Omar K. Khalique[1†], Raymond Lee[2], Isaac Y. Wu[3], Hyde Russell[4], Mayra Guerrero[5], Dee Dee Wang[6], Ramesh Veeragandham[7], Ashequl M. Islam[8], David W. Deaton[9], Tsuyoshi Kaneko[10], Kyle W. Eudailey[11], Deniz Akkoc[1], Alex Kantor[1], Catherine Wang[1], Diane C. H. Tang[1], Joongheum S. Park[1], Diana Leung[1], Tamim M. Nazif[1], Torsten P. Vahl[1], Rebecca T. Hahn[1], Susheel K. Kodali[1], Martin B. Leon[1], Hiroo Takayama[1], Vinayak Bapat[1], Michael A. Borger[12], and Isaac George[1]*

[1]Division of Cardiology, New York-Presbyterian Hospital, Columbia University Medical Center, MHB 7GN-435, 177 Ft Washington Ave, New York, NY 10032, USA; [2]Division of Cardiothoracic Surgery, Cardiovascular Thoracic Institute, University of Southern California, Santa Monica, CA, USA; [3]Department of Anesthesia, New York-Presbyterian Hospital, Columbia University Medical Center, MHB 7GN-435, 177 Ft Washington Ave, New York, NY 10032, USA; [4]Division of Cardiothoracic Surgery, Evanston Hospital Northshore University HealthSystem, Evanston, IL, USA; [5]Division of Cardiology, Mayo Clinic Hospital, Rochester, MN, USA; [6]Division of Cardiology, Henry Ford Hospital Center for Structural Heart Disease, Detroit, MI, USA; [7]Division of Cardiothoracic Surgery, John Muir Health Care, Concord, CA, USA; [8]Division of Cardiology, Baystate Medical Center, Springfield, MA, USA; [9]Division of Cardiothoracic Surgery, Baystate Medical Center, Springfield, MA, USA; [10]Division of Cardiothoracic Surgery, Brigham and Women's Hospital, Boston, MA, USA; [11]Princeton Baptist Medical Center, Birmingham, AL, USA; and [12]Department of Cardiac Surgery, Leipzig Heart Center, Leipzig, Germany

Received 28 December 2018; editorial decision 4 March 2019; accepted 6 March 2019

Aims To investigate valve sizing and the haemodynamic relevance of the predicted left ventricular outflow tract (LVOT) in patients with mitral annular calcification (MAC) undergoing transatrial transcatheter valve implantation (THV).

Methods and results In total, 21 patients undergoing transatrial THV, multiplanar reconstruction (MPR), maximum intensity projection (MIP), and cubic spline interpolation (CSI) were compared for MA sizing during diastole. In addition, predicted neo-LVOT areas were measured in 18 patients and correlated with the post-procedural haemodynamic dimensions. The procedure was successful in all patients (100%). Concomitant aortic valve replacement was performed in eight patients (43%) (AVR group). Sizing using MPR and MIP yielded comparable results in terms of area, perimeter, and diameter, whereas the dimensions obtained with CSI were systematically smaller. The simulated mean systolic neo-LVOT area was $133.4 \pm 64.2\,mm^2$ with an anticipated relative LVOT area reduction (neo-LVOT area/LVOT area $\times$ 100) of $59.3 \pm 14.7\%$. The systolic relative LVOT area reduction, but not the absolute neo-LVOT area, was found to predict the peak ($r = 0.69$; $P = 0.002$) and mean ($r = 0.65$; $P = 0.004$) post-operative aortic gradient in the overall population as well as separately in the AVR (peak: $r = 0.91$; $P = 0.002$/mean: $r = 0.85$; $P = 0.002$) and no-AVR (peak: $r = 0.89$; $P = 0.003$/mean: $r = 0.72$; $P = 0.008$) groups.

Conclusion In patients with severe MAC undergoing transatrial transcatheter valve implantation, MPR, and MIP yielded comparable annular dimensions, while values obtained with CSI tended to be systematically smaller. Mitral annular area and the average annular diameter appear to be reliable parameters for valve selection. Simulated relative LVOT reduction was found to predict the post-procedural aortic gradients.

* Corresponding author. Tel: 1-212-305-4134; Fax: 1-646-426-0156. E-mail: ig2006@cumc.columbia.edu

† These authors contributed equally to this work.

Keywords transcatheter mitral valve replacement • mitral annular calcification • mitral regurgitation • mitral stenosis • valvular heart disease • computed tomography

Introduction

Mitral annular calcification (MAC) is present in 8–15% of the elderly population.[1] As populations grow older, symptomatic mitral valve (MV) disease in conjunction with severe concentric annular calcification is becoming more common and substantially complicates surgical MV replacement. For this reason, transcatheter balloon-expandable valve implantation into the calcified annulus has been investigated.[2] Growing experience shows that a high proportion of MAC patients are not suitable for the transseptal or transapical access due to increased risk of obstruction of the left ventricular outflow tract (LVOT). Alternative strategies for preventing LVOT obstruction (LVOTO) include intentional percutaneous laceration of the anterior mitral leaflet (LAMPOON),[3] alcohol septal ablation,[4] and the use of the hybrid transatrial access. Principle advantages of the transatrial compared to the transseptal or transapical approaches include the systematic resection of the anterior MV leaflet, valve sizing and implantation under direct visualization, and adjunctive techniques aiming to prevent paravalvular leaks.[5–7]

All approaches require precise imaging for mitral annulus (MA) sizing and assessment of the neo-LVOT in order to estimate the risk of LVOTO, which has been described in more than 10% of patients undergoing valve-in-MAC procedures.[2] No data exist about the technique for sizing the mitral annulus in patients with MAC. Valve simulation on computed tomography (CT) images or 3D printing have been proposed for risk evaluation and pre-procedural planning.[8,9] Data regarding the haemodynamic relevance of the neo-LVOT are limited.

In this study, we aim to determine the most appropriate sizing strategy in MAC patients undergoing transatrial transcatheter valve implantation (THV) at six North American centres and to investigate the haemodynamic relevance of the predicted change in LVOT obtained by valve simulation on CT.

Methods

Patients

Patients with severe MAC and either severe mitral stenosis (MS), mitral regurgitation (MR), or mixed disease included into a multicentre registry investigating the outcomes of transatrial implantation of a balloon-expandable THV were considered for this analysis. Severe MAC was defined as a concentric calcification of the MA involving both the anterior and the posterior leaflet over more than two-thirds of the circumference.

Exclusion criteria included insufficient quality of the pre-procedural cardiac CT and untreated severe aortic stenosis in one patient. The decision of eligibility for treatment via the transatrial approach was based on the judgement of the institutional Heart Team. The following criteria were considered to support the use of the transatrial approach: increased predicted risk of LVOTO, non-concentric calcifications or large annular diameter increasing the risk of valve embolization, and the presence of extensive calcifications of the subvalvular apparatus, possibly interacting with the delivery system during a percutaneous approach. Clinical, procedural, and outcomes data were collected prospectively, whereas imaging studies were analysed retrospectively. The study was approved by the Institutional Review Board and follows the requirements of the Declaration of Helsinki.

Procedure and surgical valve sizing

Implantation of a balloon-expandable THV was performed on cardiopulmonary bypass via left atrial exposure as shown in *Figure 1* and as previously described.[7] The anterior MV leaflet was systematically resected and pledgeted sutures were placed to enhance stability and minimize the risk of paravalvular leak. Final decision on valve selection was made during surgery based on direct inspection of the MV and balloon sizing. In the majority of patients, post-dilatation of the valve was performed, generally with the addition of supplemental volume into the implantation balloon.

Image acquisition

Transthoracic echocardiography

All patients underwent transthoracic echocardiography at baseline and discharge in order to determine the severity of MV disease, record transvalvular, and LVOT gradients. Symptomatic patients with a MV area <1.5 cm^2 and a mean gradient >5 mmHg and/or moderate to severe MR were considered eligible for the intervention.[10] Patients were classified in the mixed disease group if they had both moderate MS and moderate to severe MR. Patients were divided into two groups according to whether concomitant aortic valve replacement was performed (AVR group) or not (no AVR group). Continuous wave (CW) Doppler through LVOT and aortic valve were used to measure the highest velocity before and after transatrial MV replacement. Peak and mean gradients were calculated based on the recorded signal and compared.

Transoesophageal echocardiography

In a subgroup of patients, 3D volumes were acquired in the operating room immediately after valve implantation for analysis of valve expansion. Area and perimeter of the implanted THV were measured at the inflow and the level of the MA using a commercially available software enabling semi-automated indirect planimetry (Qlab Mitral Valve Navigator Version 10.0; Philips, Amsterdam, The Netherlands).

Cardiac CT

An example of a typical cardiac CT protocol and the imaging methods used are available in the Supplementary data online. The mitral module of the 3-mensio quantification software (Pie Medical, Maastricht, Netherlands) was used for all annular and LVOT measurements.

For annulus sizing, the inner borders of the calcium within the MA were traced during diastole (70–80% dependent on image quality) to minimize motion artefact using three different methods:

(1) Multiplanar reconstruction (MPR) of a short-axis view (*Figure 2A* and *B*): the plane was aligned with the annular calcium in two different views. The images were windowed in order to optimize enhancement of the calcium. Accounting for non-planar distribution of the calcium, the reformation plane was then moved longitudinally in the atrial and ventricular dimension to obtain a plane with

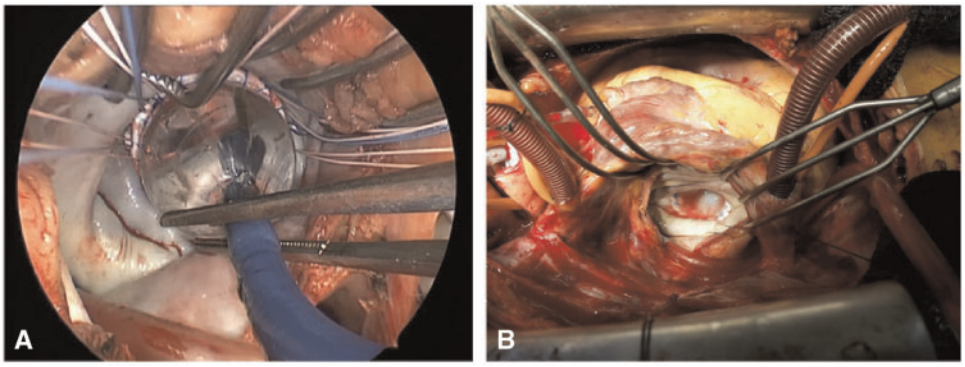

Figure 1 Transatrial implantation of a balloon-expandable valve in the mitral position. (*A*) The mitral valve is exposed through a left atriotomy, and the transcatheter heart valve is deployed under direct visualization. Pledgeted sutures have been previously placed in order to minimize the risk of paravalvular regurgitation. (*B*) Final result.

circumferential distribution of calcium thought to represent the calcific anchoring plane of the transcatheter valve.

(2) Cubic spline interpolation (CSI; *Figure 2C* and *D*): the maximally protruding borders of the calcium were manually tracked by placing 16 segmentation points by automated stepwise rotation of a long-axis view aligned to the long axis of the left ventricle. For non-calcified portions, the leaflet-annulus hinge points were identified. Minimal and maximal diameters were measured manually.

(3) Maximum intensity projection (MIP) (*Figure 2E*): MIP was orientated to minimize foreshortening. This was achieved through positioning of the volume in a way allowing complete discrimination without overlap between the mitral annulus and the (generally calcified) aortic valve, similarly to a surgical view on echocardiography in order to obtain the true maximum dimensions of the annulus. The annulus was directly traced on the reconstructed image.

Truncation of the anterior horn of the saddle-shaped annulus (creating a D-shaped annulus) was exclusively used in the absence of anterior annular calcium, otherwise the annular calcium was followed.

LVOT and neo-LVOT measurements

In patients with sufficient imaging quality, aortic root and LVOT were reconstructed during mid-systole (35%) using the dedicated algorithms (*Figure 3A* and *B*). Particular attention was paid to carefully adjust the centreline in the middle of the LVOT. The implanted valve was simulated according to the nominal manufacturer frame size in a way that mimicked the surgical valve implantation, whereby 80% of the virtual frame was localized in the ventricle and 20% (3–4 mm) in the left atrium. Following the LVOT centreline, LVOT and neo-LVOT areas at the level of maximal valve protrusion were measured. The relative LVOT reduction defined as (LVOT area - neo-LVOT (at the same level)/LVOT area) × 100 was then calculated and correlated to the aortic gradients obtained by CW Doppler measurement across the aortic valve.

Calcium volume

For calculation of the mitral calcium volume, the MV was manually identified using the aortic module in an off-label fashion. Contrast enhancement of the left atrium was measured, and an individual cut-off was defined for each patient by adding 150 Hounsfield units to the obtained value. The identification window was manually adjusted in order to include the entire MV complex (Supplementary data online, *Figure S1*).

Statistical analysis

Statistical analyses were performed using IBM SPSS version 21 (IBM, Armonk, NY, USA). Statistical significance was assumed for $P < 0.05$. Continuous variables are reported as mean ± standard deviation. Normality of distributions for continuous variables was tested using the Shapiro–Wilk test. Comparisons between methods were performed using a paired two-sided Student's *t*-test. Pearson correlation coefficients and multiple regression were used to assess the correlations between measurements from echocardiography and CT. Intraclass correlation coefficients were used to assess interobserver reproducibility between readers (F.P. and O.K.K.), using a two-way mixed-model absolute-agreement method. Both readers were blinded to the previous MA and neo-LVOT measurements that were repeated in all patients. Reproducibility of all reported correlations and analyses were confirmed independently using the data of each observer.

Results

Study population

The images of 26 consecutive patients with MAC referred for transatrial implantation of a balloon-expandable THV at six centres were systematically reviewed. The study flowchart is shown in Supplementary data online, *Figure S2*. Twenty-one patients had a CT scan allowing for diastolic MA sizing and calcium volume analysis were included. Among them, 18 patients had sufficient CT quality enabling valve simulation and reconstruction of the neo-LVOT, and a subgroup of nine patients had post-procedural 3D transoesophageal echocardiography (TOE) volumes of the implanted valve available for the assessment of stent frame dimensions.

Clinical and functional characteristics

The clinical baseline characteristics of the 21 patients with severe MAC included into this study are summarized in the Supplementary data online, *Table S1*. According to baseline echocardiographic assessment, 11 patients (52%) had predominant MS, 6 (29%) predominant MR, and 4 (19%) had mixed MV disease. Eight patients (43%) presented with significant aortic valve disease requiring concomitant aortic valve replacement (AVR); aortic stenosis in seven cases and aortic regurgitation in one case. One patient already had a normally

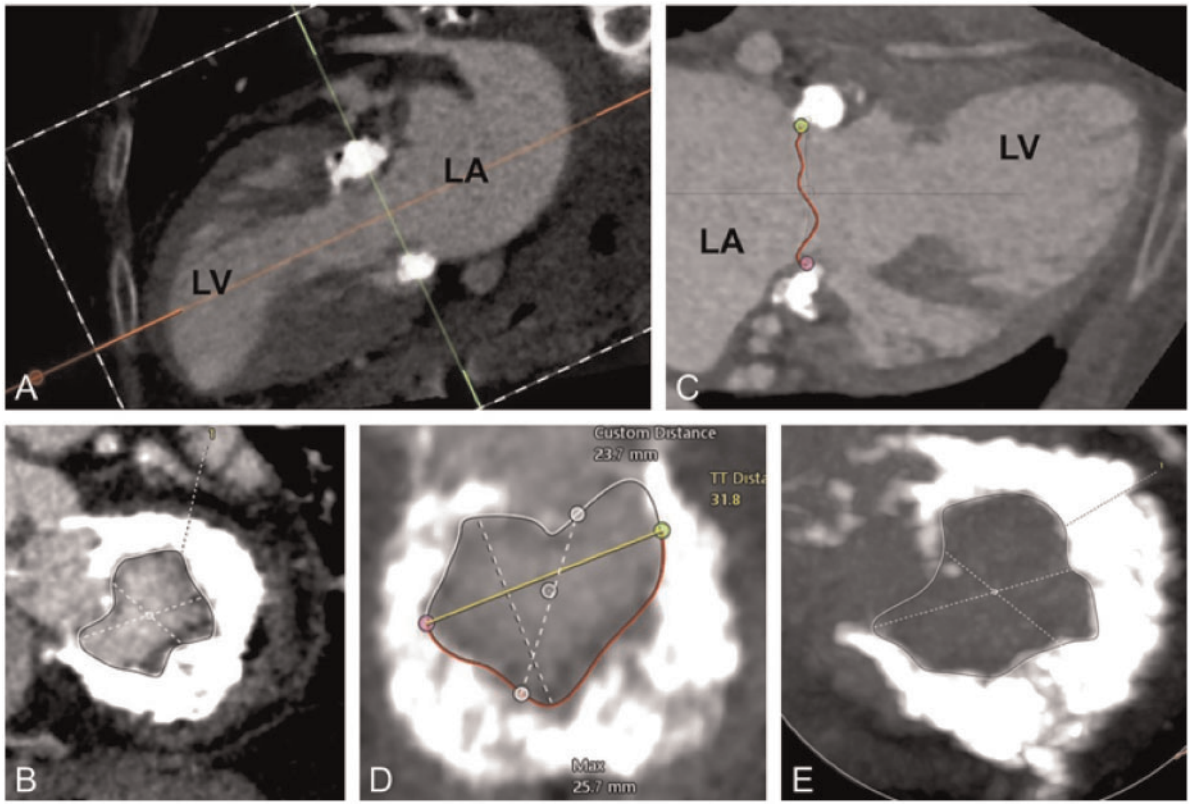

Figure 2 The three imaging methods used for annular sizing. (*A*) MPR; (*B*) CSI used for delineation of the inner calcium contours; (*C*) MA area measured by MPR. (*D*) Annular area obtained with CSI; (*E*) Annulus area assessed using maximum intensity projection. LA, left atrium; LV, left ventricle.

functioning surgical AVR in place. The echocardiographic characteristics are listed in Supplementary data online, *Table S2*.

Anatomic characteristics

The results of the diastolic MA measurements performed on the preoperative cardiac CT images using MPR, MIP, and CSI are listed in *Table 1*. MA anatomy differed significantly according to the predominant MV disease aetiology. Patients with predominant MR presented with significantly larger MA area, perimeter, and diameters compared to those with predominant MS. Patients with mixed disease had intermediate dimensions. In contrast, the mitral calcium volume, which was highly elevated in all patients (mean 6528 ± 3863 mm^3; range: 1504–13 781 mm^3), did not significantly differ between groups.

The mean predicted neo-LVOT area based on valve simulation was 133.3 ± 66.4 mm^2 with a relative LVOT reduction of 59.3 ± 14.7%, consistently indicating high risk of LVOTO of the selected patients. Importantly, no significant differences were found in LVOT dimensions according to the predominant aetiology of MV disease.

Annulus sizing

MPR and MIP yielded comparable results in terms of area, perimeter, and diameters, whereas dimensions obtained with CSI were systematically smaller with regards to area, projected perimeter, and maximal diameter. Conversely, no statistically significant differences were found between CSI 3D perimeters and minimal MA diameters and the corresponding measurements obtained with MPR and MIP. The corresponding Bland–Altman plots for area, perimeter, and average diameter are shown in *Figures 3–6*. Reproducibility was excellent for all methods with interclass coefficients for interobserver agreement ranging from 0.90 to 0.96 (Supplementary data online, *Table S3*).

Procedural results

Two patients (10%) received an Edwards Sapien XT, and 19 (90%) an Edwards Sapien 3 bioprosthesis. A mean extra volume of 2 ± 1 mL was added in almost every patient either during implantation or post-dilation. Concomitant AVR was performed in eight patients (38%) and septal surgical myectomy in two patients. The mean transmitral gradient decreased from 11 ± 6 to 4 ± 2 mmHg ($P < 0.001$) with trace or mild MR in all patients. Thus, technical success according to the criteria of the Mitral Valve Academic Research Consortium (MVARC) was achieved in all patients. LVOTO was observed in one patient—this patient had a systolic predicted neo-LVOT of 48 mm^2, relative area reduction of 83%, and leading to a post-procedural mean aortic gradient of 30 mmHg. The patient was treated conservatively, though she later died of respiratory failure. Two additional patients had an increase of their mean aortic gradient of >10 mmHg that did not translate into clinical symptoms.

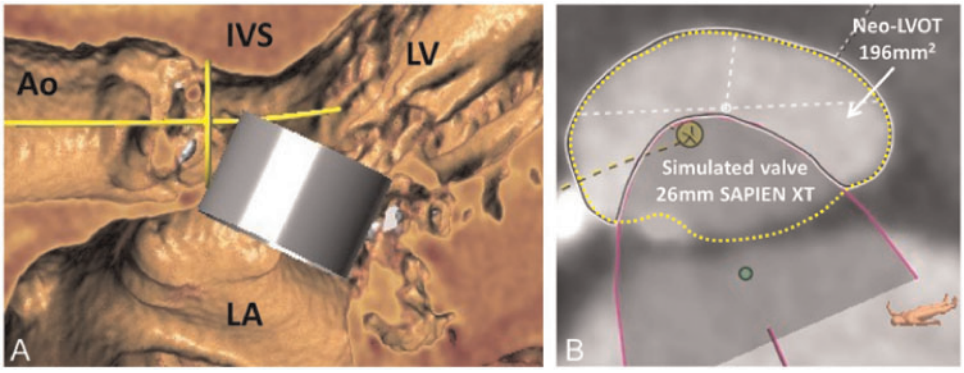

Figure 3 Principle of valve simulation and prediction of neo-LVOT. (*A*) Virtual valve implantation (Edwards Sapien 3 26 mm) using a cylinder corresponding to the nominal dimensions of the THV. (*B*) Measurements of the LVOT (interrupted yellow line) and neo-LVOT area (white continuous line) at the level of maximal valve protrusion. Ao, aorta; IVS, interventricular septum; LA, left atrium; LV, left ventricle.

Table 1 Measurements by cardiac CT according to mitral valve disease aetiology

	All (*N* = 21)	Predominant MS (*N* = 11)	Predominant MR (*N* = 6)	Mixed disease (*N* = 4)	*P*-value[a]
Direct planimetry (CT_MPR)					
MA area (mm^2)	530.9 ± 177.3	429.0 ± 106.5	734.7 ± 165.2	505.2 ± 64.2	<0.001
MA perimeter (mm)	88.9 ± 13.1	81.3 ± 10.2	102.8 ± 10.1	88.9 ± 5.6	<0.001
MA maximal diameter (mm)	31.4 ± 4.8	28.2 ± 3.0	36.5. ± 3.8	32.5 ± 2.8	<0.001
MA minimal diameter (mm)	20.1 ± 5.1	17.6 ± 4.3	25.1 ± 4.5	19.6 ± 1.4	0.004
Maximum intensity projection (CT_MIP)					
MA area (mm^2)	520.2 ± 156.2	419.0 ± 114.7	708.4 ± 156.2	549.3 ± 61.7	<0.001
MA perimeter (mm)	88.0 ± 12.8	80.4 ± 11.8	99.4 ± 10.2	92.8 ± 2.8	0.005
MA maximal diameter (mm)	31.4 ± 4.5	29.1 ± 4.2	34.4 ± 3.8	33.6 ± 2.0	0.02
MA minimal diameter (mm)	20.1 ± 4.6	17.7 ± 3.8	24.9 ± 3.4	19.8 ± 2.4	0.002
Cubic spline interpolation (CT_CSI)					
MA area (mm^2)	496.7 ± 181.0	399.1 ± 120.0	698.3 ± 151.3	492.5 ± 95.4	<0.001
MA 3D perimeter (mm)	88.3 ± 15.2	81.5 ± 14.0	102.3 ± 10.4	90.3 ± 11.3	0.006
MA projected perimeter (mm)	84.9 ± 14.6	78.6 ± 13.9	98.9 ± 10.3	86.2 ± 9.1	0.007
MA maximal diameter (mm)	29.0 ± 5.4	26.5 ± 5.0	34.1 ± 3.3	30.6 ± 3.5	0.005
MA minimal diameter (mm)	20.0 ± 4.5	16.9 ± 3.4	24.7 ± 2.8	19.3 ± 1.3	<0.001
MA calcium volume (mm^3)	6528 ± 3863	6369 ± 3810	8756 ± 4180	3619 ± 804	0.25
Anterior leaflet	629 ± 414	694 ± 474	580 ± 430	538 ± 272	0.64
Posterior leaflet	5929 ± 3752	5738 ± 3673	8176 ± 4053	3082 ± 660	0.23
Systolic LVOT and neo-LVOT dimensions					
LVOT (mm^2)	322.1 ± 73.6	309.8 ± 77.8	376.7 ± 71.2	301.4 ± 19.1	0.16
Neo-LVOT (mm^2)	133.4 ± 64.2	133.3 ± 66.4	156.8 ± 76.2	96.7 ± 36.7	0.57
Absolute LVOT area reduction (mm^2)	188.7 ± 51.7	176.5 ± 51.7	220.2 ± 55.0	204.7 ± 45.2	0.18
Relative LVOT reduction (%)	59.3 ± 14.7	57.9 ± 15.8	59.1 ± 14.3	65.1 ± 15.0	0.90

CSI, cubic spline interpolation; CT, computed tomography; MA, mitral annulus; MIP, maximum intensity projection; MPR, multiplanar reconstruction; MR, mitral regurgitation; MS, mitral stenosis.
[a]*P*-values compare patients with MS to patients with MR.

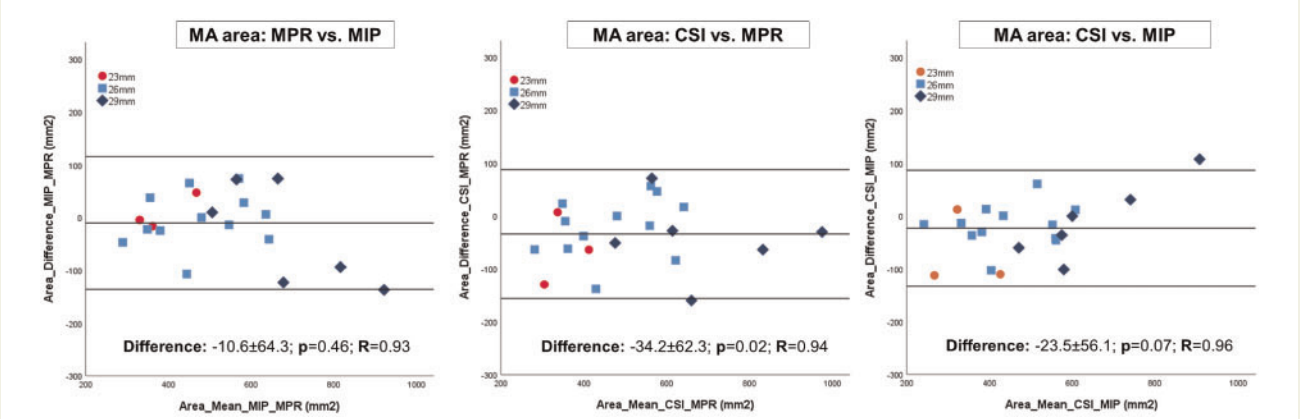

Figure 4 Bland–Altman plots for the comparison between the different methods for measurement of MA area.

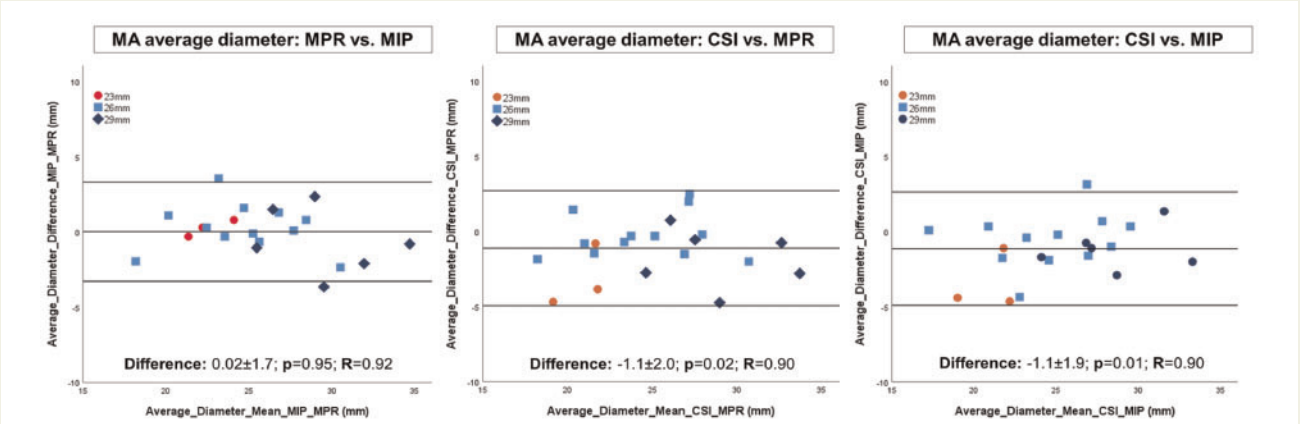

Figure 5 Bland–Altman plots for the comparison between the different methods for measurement of MA average diameter.

Valve sizing

Valve selection under direct visualization and balloon sizing resulted into the implantation of a 29 mm Sapien THV in six patients, a 26 mm in 12 patients, and a 23 mm in three patients.

Anatomic characteristics according to valve size expressed as median and interquartile range are listed in *Table 2*. Calculation of the average diameter ($= maximal\ diameter + minimal\ diameter \div 2$) and the area-derived diameter ($= 2x\sqrt{annular\ area \div \pi}$) yielded comparable results.

Compared to area-based sizing recommended by the manufacturer for aortic implantation of the Edwards Sapien 3 valve, three patients received a manifestly oversized valve after surgical inspection. Among them, a negative clinical impact was observed in only one patient in the form of LVOTO, probably related to protrusion of the covered valve stent portion into the LVOT.

Valve expansion

Stent frame areas and perimeters measured by TOE using semi-automated indirect planimetry are shown in the table of Supplementary data online, *Figure S3*. Due to shadowing induced by the transcatheter heart valve, the outflow (on the ventricular side) could not be assessed in any patients. The analysis of valve expansion yielded the following results: (i) a larger valve area at the inflow or atrial part (481.4 ± 91.5 mm^2) was observed compared to the portion of the frame at the level of the calcified annulus (412.3 ± 80.4 mm^2); (ii) irrespective of the method used for MA sizing, the area of the mid-portion of the implanted THV did not exceed the anatomic annular area measured on the CT images; and (iii) valve expansion (assessed as the difference between the areas and perimeters of the mid-portion and the inflow of the THV) was optimized with extra volume added (above nominal volume) during post-dilatation (Supplementary data online, *Figures S3* and *S4*).

Haemodynamic relevance of the predicted neo-LVOT

CW Doppler across the aortic valve at baseline according to the presence or not of concomitant aortic valve disease are listed in *Table 3* After valve implantation, the peak and mean aortic gradients in the

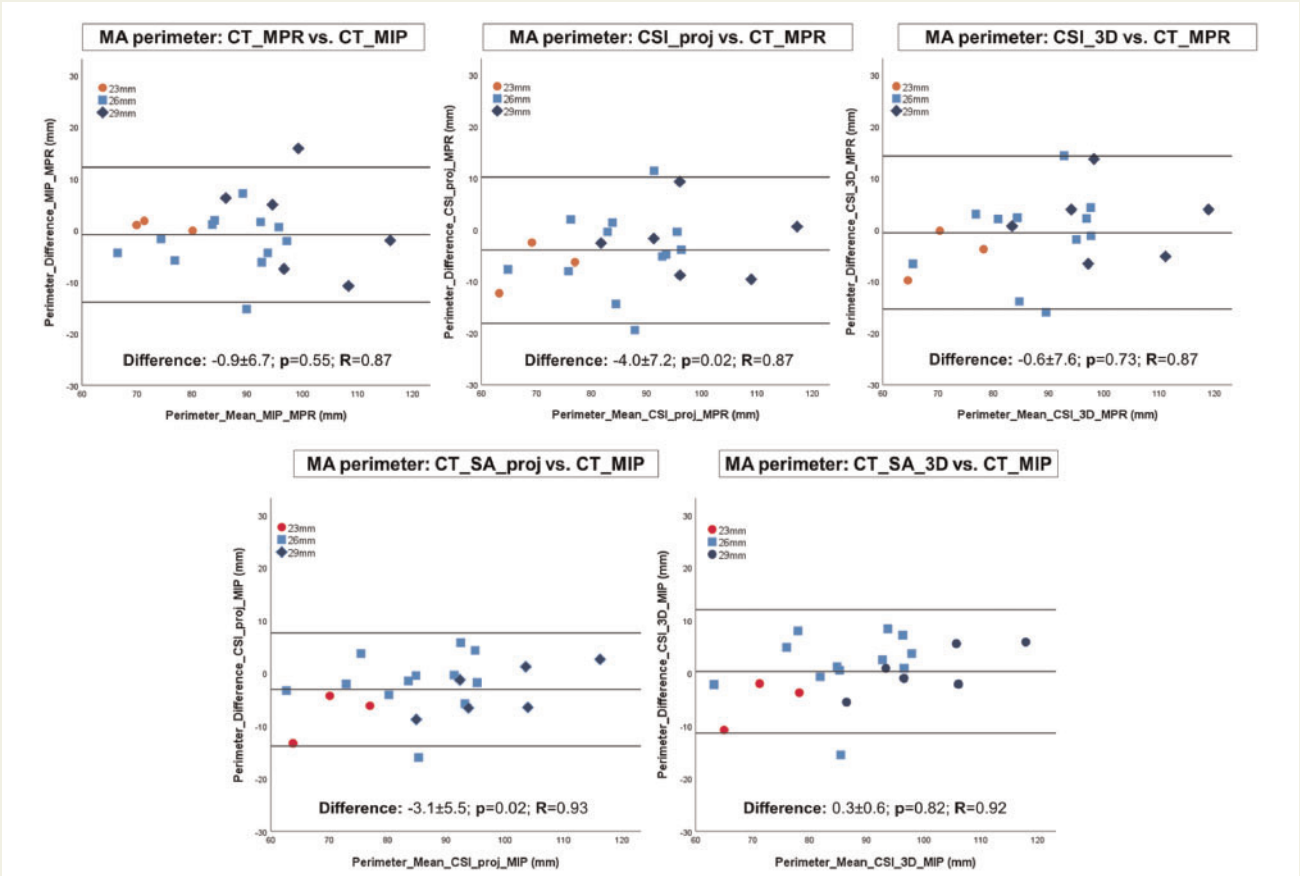

Figure 6 Bland–Altman plots for the comparison between the different methods for measurement of MA perimeter.

patients who underwent concomitant aortic valve replacement were 27 ± 13 and 14 ± 8 mmHg, respectively, whereas they were 23 ± 9 and 11 ± 4 mmHg, respectively, in the patients without AVR. While the aortic gradients decreased in the patients with aortic valve disease at baseline following concomitant aortic valve replacement (Δpeak gradient: -41 ± 42 mmHg and Δmean gradient: -19 ± 24 mmHg), an increase was observed in the no-AVR group after transatrial MV implantation (Δpeak gradient: 9 ± 11 mmHg, and Δmean gradient: 4 ± 5 mmHg). Applying multiple regressions, the systolic relative LVOT area reduction and the presence of a surgical aortic valve in aortic position were found to predict the peak and mean postoperative aortic gradients. The corresponding correlations for the overall cohort as well as for both the AVR and the no-AVR groups are shown in *Figure 7*.

The relative reduction of the LVOT area also predicted the absolute change of the aortic gradients (defined as aortic gradient after minus before the procedure) in the patients without aortic valve disease at baseline (Supplementary data online, *Figure S5*). A relative LVOT reduction of 60% corresponded to an increase of the mean and peak aortic gradients by about 3 and 7 mmHg, respectively, whereas a relative LVOT reduction of 80% increased the mean and peak aortic gradient by 8.5 and 19.5 mmHg, respectively.

Interobserver agreement assessed with intraclass correlation coefficients for the measurement of the neo-LVOT and relative LVOT reduction were 0.98 and 0.91, respectively.

Discussion

The main findings of our study can be summarized as follows: (i) annular dimensions in patients with severe MAC differ according to the aetiology of MV disease; (ii) MPR, MIP yielded comparable, and reliable results for the measurements of the annular dimensions, whereas dimensions obtained with CSI were systematically smaller, except for 3D perimeter; (iii) rather than absolute values, the relative systolic LVOT reduction was found to predict the post-procedural aortic gradients in patients undergoing transatrial MV implantation; (iv) despite routinely performed post-dilation, there is no evidence that valve expansion beyond the pre-procedural annulus dimension measured by CT occurred, though post-dilatation resulted in improved stent frame expansion.

Imaging methods for annulus sizing

The best agreement between imaging methods was found for MPR and MIP that yielded statistically comparable values for all considered parameters. Conversely, the dimensions obtained with the semi-automated CSI method were systematically smaller, except for the 3D perimeter (in contrast to the projected perimeter). These discrepancies are likely explained by identification of the calcium protruding into the annulus in several planes using the CSI method, finally resulting in a smaller area.

Table 2 CT anatomic characteristics according to the implanted valve size expressed as median and interquartile range

Parameters	23 mm	26 mm	29 mm
Direct planimetry (CT_MPR)			
MA area (mm^2)	369.7 (351.3–406.8)	489.0 (384.0–557.2)	624.2 (553.1–681.9)
MA perimeter (mm)	70.4 (69.9–75.3)	88.6 (82.3–95.8)	95.3 (93.5–103.8)
MA maximal diameter (mm)	28.0 (25.4–28.2)	30.4 (29.1–32.3)	34.8 (31.6–38.0)
MA minimal diameter (mm)	19.1 (17.6–19.7)	18.6 (15.1–20.2)	24.8 (21.3–27.2)
MA area-derived diameter (mm)	21.7 (21.1–22.7)	24.9 (22.1–26.6)	29.5 (26.5–32.5)
MA average diameter (mm)	22.1 (21.8–22.9)	24.6 (22.1–26.1)	29.6 (26.5–32.6)
Maximum intensity projection (CT_MIP)			
MA area (mm^2)	352.9 (340.5–421.9)	481.5 (372.2–599.1)	616.5 (600.5–701.7)
MA perimeter (mm)	72.2 (71.3–76.1)	87.3 (80.1–92.8)	99.4 (92.2–108.0)
MA maximal diameter (mm)	26.7 (25.5–28.1)	31.4 (29.7–32.4)	34.1 (33.8–35.7)
MA minimal diameter (mm)	18.2 (16.7–20.3)	19.9 (15.9–21.9)	24.0 (19.0–26.8)
MA area-derived diameter (mm)	21.2 (20.8–23.1)	24.8 (21.8–27.6)	29.0 (27.2–30.9)
MA average diameter (mm)	22.4 (21.8–23.4)	25.3 (23.2–27.5)	28.9 (27.3–30.7)
Cubic spline interpolation (CT_CSI)			
MA area (mm^2)	340.0 (290.0–360.0)	430.0 (357.5–582.5)	600.0 (575.0–707.5)
MA 3D perimeter (mm)	70.2 (64.9–73.3)	85.5 (80.7–97.2)	100.5 (94.4–107.6)
MA projected perimeter (mm)	67.9 (62.5–70.9)	83.6 (77.2–91.9)	96.1 (90.7–103.2)
MA maximal diameter (mm)	22.1 (20.4–22.9)	29.1 (26.7–32.3)	32.4 (30.0–35.3)
MA minimal diameter (mm)	17.6 (16.3–18.3)	20.4 (17.0–21.8)	23.2 (20.5–25.8)
MA area-derived diameter (mm)	21.3 (20.8–23.4)	23.4 (21.3–27.2)	27.6 (27.3–30.8)
MA average diameter (mm)	21.3 (19.9–24.1)	24.3 (21.0–26.6)	26.9 (26.5–31.0)

According to Bland–Altman analysis, area measurement appears overall more reproducible than perimeter in this particular setting. Indeed, our experience shows that perimeter may be very variable between techniques due to the complexity of the calcification pattern. Measurement of diameter appears particularly reproducible using the MPR and MIP techniques. With the Sapien valve system, the MA is forced to adopt a more circular shape during balloon expansion. As expected with an irregularly-shaped annulus, perimeter measurements will result in gross over-estimations of average annular area (Supplementary data online, *Figure S6*). Thus, sizing recommendations should focus on area and average diameters rather than perimeter in this disease process. As there may be a risk of underestimating annular dimensions with CSI, MPR, or MIP methods may be preferred due to simplicity and availability in all radiology software programmes. Further advantages and limitations of the different imaging methods are listed in *Table 4*.

Anatomic characteristics

Our study is the first to report anatomic variations in patients with severe MAC according to the predominant aetiology of MV disease. Because of the homogeneity of the population included into this analysis (95% of women with preserved left ventricular ejection fraction), these findings are unlikely to be explained by differences in baseline characteristics. Importantly, the observed anatomic discrepancies were not related to a lower severity of annular calcification. Specific patterns of leaflets involvement may result in the phenotype of MR rather than MS and promote annular dilatation or, conversely, the development of MR may be secondary to annular dilatation and correspond to a more advanced stage of the disease. Indeed, prior research using 3D echocardiographic imaging of the MA in patients with MAC has shown a reduction in systolic mitral annular contraction and increasing in systolic leaflet tenting as compared to controls, both of which are potential substrates for MR.[11] In line with these findings, we found only minimal differences between diastolic and systolic values.

Valve selection in MAC patients undergoing transatrial valve implantation

With intraoperative direct visualization of the MA, final valve selection in patients undergoing transatrial THV implantation was mainly based on direct surgical and balloon sizing. As a result, useful information can be derived about the relevance of anatomical CT measurements. Compared to the aortic position, area-based sizing yielded similar results except for slightly lower range limits for 23 and 26 mm valve, accounting for a higher degree of oversizing. Despite the individual anatomic variability, the average diameter was found to reliably approximate the area-derived diameter and thus, should be considered an useful parameter for sizing in addition to area.

In analogy to the sizing method proposed in patients without severe MAC,[12] D-shape truncation was performed in the patients without calcification of the aorto-mitral curtain, whereas anterior annulus

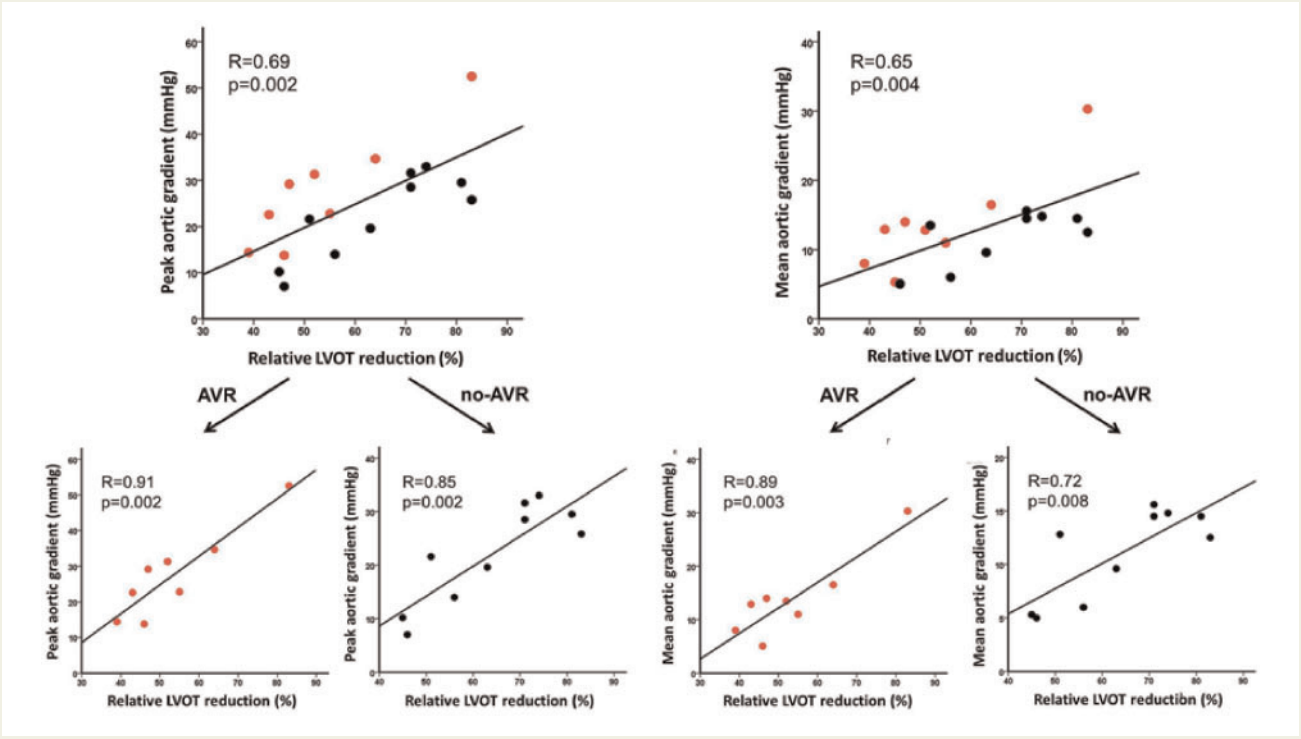

Figure 7 Haemodynamic relevance of the neo-LVOT. Relationship between the relative LVOT reduction and the peak and mean post-procedural aortic gradients in patients with and without aortic valve replacement. AVR, aortic valve replacement; LVOT, left ventricular outflow tract.

Table 3 Haemodynamic parameters determined by transthoracic echocardiography before and after mitral valve implantation

	Pre-procedural		Post-procedural			
	Significant aortic disease (*N* = 9)	No aortic disease (*N* = 12[a])	AVR (*N* = 9[b])	No AVR (*N* = 12)	Change AVR (post-pre)	Change no AVR (post-pre)
CW Doppler across the aortic valve						
Mean gradient (mmHg)	29 ± 21	8 ± 3	14 ± 7	11 ± 4	-19 ± 24	4 ± 5
Peak gradient (mmHg)	60 ± 39	14 ± 6	28 ± 13	22 ± 9	-41 ± 42	9 ± 11

AVR, aortic valve replacement; CW, continuous wave; *N*, number of patients.
[a]Including one patient with a bioprosthetic aortic valve already in place.
[b]Including the above-mentioned patient with previous AVR. One patient left with untreated aortic stenosis was excluded from the post-procedural analysis. The patient underwent TAVR 6 months after transatrial mitral valve replacement.

calcium contours (not anterior leaflet calcium) were followed in the others as already described by other groups.[13,14] Although obtained in a limited number of patients, the analysis of the post-interventional 3D TOE volumes of the implanted valve seems to support this approach, as valve expansion beyond the pre-procedural annular dimensions measured by CT did not occur in any case. Moreover, the full extent of valve oversizing expected with the addition of volume to the implantation balloon (as described for the aortic position[15]) was not reached in any patients. This suggests that the inclusion of the aorto-mitral curtain would have led to excessive oversizing and potential catastrophic consequences in terms of posterior annular disruption and LVOTO. From an anatomic point of view, posterior and anterior calcium, and calcified fibrous trigones seem to effectively constrain the (over-) expansion of the valve. However, our findings also establish that post-dilation remains a useful step for the transatrial approach in order to optimize of the stent frame and promote apposition against the calcific annulus. Additional sealing may occur on fibrotic and thickened mitral annular regions inside the circumscribed MAC or thickened mitral leaflets in this setting.

Table 4 Advantages and limitations of the different measurement methods used for MA sizing

	Advantages	Limitations
CT_MPR	High reproducibility promoted by the use of a single planeGood visualization of non-calcified portions of the MA	Potential overestimation of the MA dimensions through omission of protruding calcium deposits localized in other planes (importance of careful plane adjustment through the most calcified region of the MA)
CT_MIP	3D superposition (summation) of the calcium deposits localized in different planes minimizing the risk to overestimate the MA dimensions	No visualization of the non-calcified borders (less adapted for sizing in patients with non-concentric/disrupted calcification patterns)
CT_CSI	Simultaneous delineation/adjustment in two different planesAccurate identification of the leaflet-annulus hinge point of the non-calcified MA portions	Potential variability in the delineation (D-shape) of the anterior segments (particularly the aorto-mitral curtain) if calcifications are lacking

CSI, cubic sline interpolation; CT, computed tomography; MA, mitral annulus; MIP, maximum intensity projection; MPR, multiplanar reconstruction.

Haemodynamic relevance of the simulated neo-LVOT

Although considered as an important parameter for the planning of transcatheter MV replacement, only limited data exist concerning the simulated neo-LVOT and its haemodynamic relevance has not been established so far. One study investigating 38 patients undergoing various transcatheter MV interventions found that an absolute neo-LVOT area ≤189.4 mm^2 was predictive of the occurrence of LVOTO as defined by an increase of 10 mmHg of LVOT invasive peak-to-peak gradient.[14] In another similar study investigating 194 patients, a simulated neo-LVOT area ≤1.7 cm^2 was found to predict LVOTO with sensitivity and specificity.[16]

The increase of the continuous-wave Doppler aortic gradients observed in the no-AVR patients after MV implantation is most likely explained by the protrusion of the uncovered stent frame into the LVOT, creating a flow acceleration with subsequent increase of the LVOT gradient, but typically no clinically apparent obstruction thanks to the resection of the anterior MV leaflet.

Importantly, our report also confirms that a certain degree of LVOTO can rarely occur despite of the resection of the anterior MV leaflet, as already described with the LAMPOON technique.[17] This most likely relates to protrusion of the part of the valve stent covered by fabric skirt into the LVOT.

The difference in the magnitude of the correlations between the AVR and the no-AVR groups (*Figure 7*) are the result of the different haemodynamic characteristics of the patients of each group. Indeed, patients with a surgical valve in aortic position naturally have higher gradients compared to those with a native valve without relevant disease. This relates to the intrinsic haemodynamic characteristics of surgical bioprostheses, including the presence of a metallic stent as well as a smaller nominal valve area. Hence, the presence of an aortic bioprosthesis was the strongest predictor of the post-procedural aortic valve gradients according to multivariate analysis followed by relative LVOT reduction, confirming that both factors determine post-procedural haemodynamics.

Our report is the first establishing a haemodynamic relationship between the simulated neo-LVOT and the post-procedural aortic gradients, supporting the use of valve simulation for pre-procedural planning. Importantly, only the relative LVOT reduction was found to predict the aortic gradients and not absolute values. These findings highlight the need to interpret the results of valve simulation individually and suggest the existence of a relative rather than an absolute cut-off.

Differences with other approaches to the MV

An algorithm summarizing the different steps of valve selection according to anatomy and access is shown in *Figure 8*. The transatrial approach offers the highest level of procedural control, while with the transseptal and transapical access the implantation depth is far less predictable. This certainly has important implications on pre-procedural planning, in particular valve simulation. Indeed, the degree of valve protrusion into the LVOT and, thus, the risk of LVOTO is largely influenced by the implantation depth. Therefore, pre-procedural neo-LVOT simulation may be more accurate and reproducible with transatrial implantation compared to other approaches. Moreover, the transatrial approach with anterior leaflet resection allows for blood flow through the ventricular end of the Sapien valve cells, which does not occur with the percutaneous approach due to the presence of the anterior mitral leaflet and a functionally covered stent frame.

Due to systematic resection of the anterior MV leaflet, the described linear relationship between the aortic gradients and the relative LVOT reduction is certainly specific for the transatrial method and not transferable to other techniques. Indeed, the cut-off for a significant increase of the aortic gradients, that correspond to a relative reduction of the native LVOT of about 60% in our study, may be much lower (probably <40–50%) for interventions sparing the anterior leaflet such as valve-in-valve or valve-in-ring procedures. Nonetheless, our study confirm that patients at high risk for LVOTO with a small predicted neo-LVOT area (<150 mm^2) can be safely treated using the transatrial approach, while they may not be eligible for a transseptal or transapical procedure.

In contrast to other approaches, the transatrial hybrid technique enables safe treatment of patients with large anatomy (up to 800 mm^2). Although, suture placement may play a role, anchoring of the valve is largely related to the radial force of apposition against the

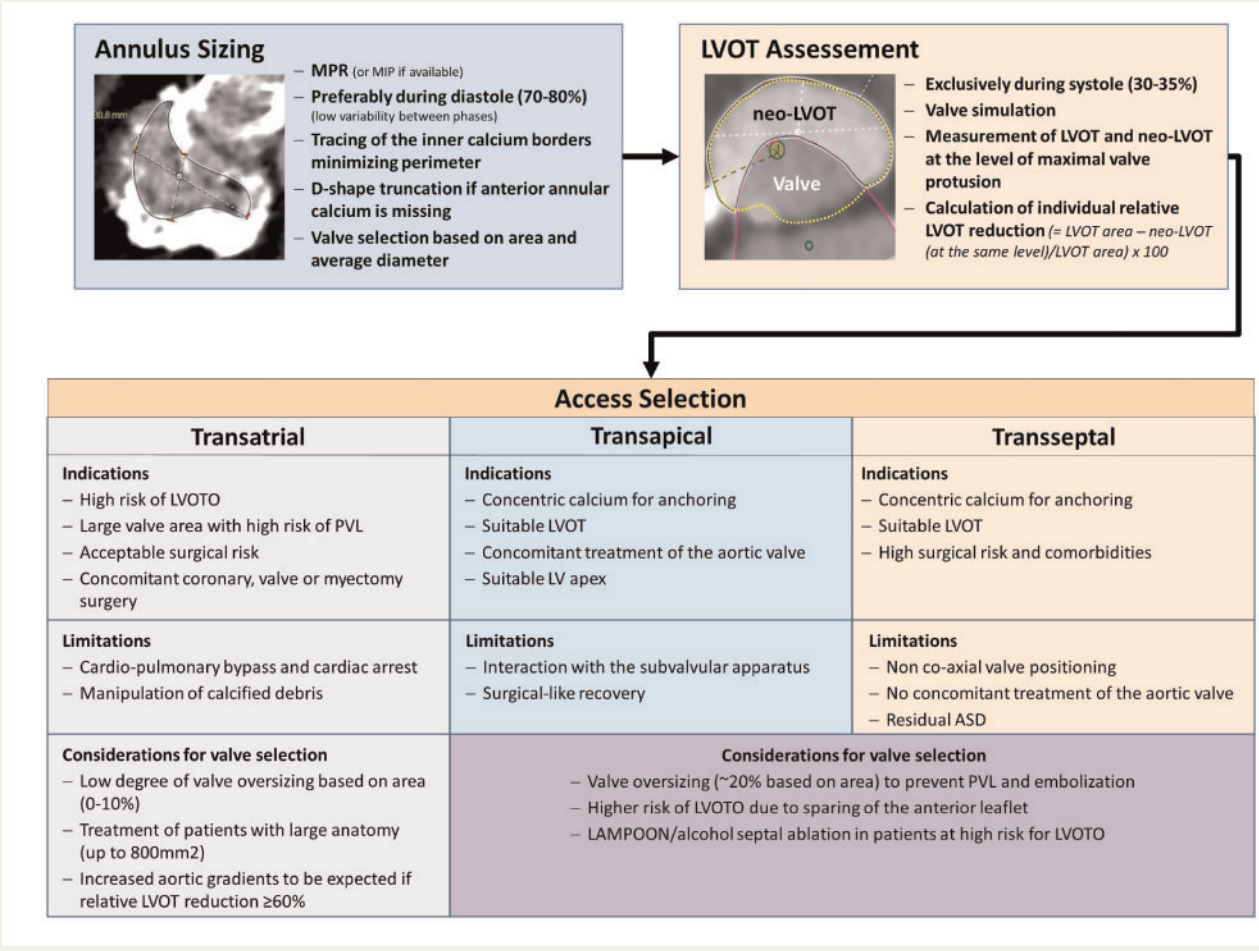

Figure 8 Algorithm for pre-procedural planning valve selection for transcatheter valve-in-MAC implantation. ASD, atrial septal defect.

calcified annulus. Despite the fact that the presented sizing strategy may not be literally translatable to other approaches (due to insufficient oversizing for the transapical and transseptal approach), we believe that some of the insights provided by our analysis will be useful for other techniques, given concentric annular calcification involving the anterior MV leaflet.

Limitations

We would like to acknowledge the following major limitations to our work. The cohort investigated in our study consists of a small number of highly selected patients with severe concentric MAC involving both MV leaflets. All patients could not undergo transseptal or transapical valve implantation due to increased risk of LVOTO or valve embolization. The anterior leaflet was systematically resected, so that the presented findings may not be translatable to other approaches.

Conclusions

In patients with severe MAC undergoing transatrial transcatheter valve implantation, we found important annular differences depending on disease aetiology. MPR and MIP yielded comparable results for the measurements of the annular dimensions, while values obtained with CSI tended to be systematically smaller. Mitral annular area and the average annular diameter were reliable parameters for valve selection. Simulated relative LVOT reduction was found to predict the post-procedural aortic gradients.

Supplementary data

Supplementary data are available at *European Heart Journal - Cardiovascular Imaging* online.

Funding

F.P. was supported by a grant from the Gottfried and Julia Bangerter-Rhyner-Foundation, Bern, Switzerland.

Conflicts of interest: F.P. is a consultant for Edwards Lifesciences; O.K.K. has received speaker fees from Edwards Lifescience; R.L. is a speaker and consultant for Abiomed; A.M.I. is a consultant for Edwards Lifesciences and Medtronic; M.G. has received research grant support from Edwards Lifescience; D.D.W. has received consulting fees for Edwards Lifesciences, Boston Scientific, and Materialise; T.K.

is a consultant for Edwards Lifesciences, Abbott, and Medtronic; R.T.H. is a consultant for Edwards Lifesciences, Gore & Associates, Medtronic, Philips Healthcare, and Siemens. S.K.K. has received research support from Edwards Lifesciences, and Medtronic, consulting fees from Claret Medical and Abbott and holds equity in Dura Biotech, and Thubrikar Aortic Valve, Inc.; V.B. is a consultant to Edwards Lifesciences, and Medtronic; M.A.B. has received speaker's honoraria and consulting fees from Edwards Lifescicences, Medtronic, CryoLife, and St. Jude; I.G. has received consulting fees for Edwards Lifesciences, Medtronic, and Boston Scientific. The remaining authors declare no conflict of interest.

References

1. Abramowitz Y, Jilaihawi H, Chakravarty T, Mack MJ, Makkar RR. Mitral annulus calcification. *J Am Coll Cardiol* 2015;**66**:1934–41.
2. Guerrero M, Urena M, Himbert D, Wang DD, Eleid M, Kodali S *et al.* 1-year outcomes of transcatheter mitral valve replacement in patients with severe mitral annular calcification. *J Am Coll Cardiol* 2018;**71**:1841–53.
3. Babaliaros VC, Greenbaum AB, Khan JM, Rogers T, Wang DD, Eng MH *et al.* Intentional percutaneous laceration of the anterior mitral leaflet to prevent outflow obstruction during transcatheter mitral valve replacement: first-in-human experience. *JACC Cardiovasc Interv* 2017;**10**:798–809.
4. Sayah N, Urena M, Brochet E, Himbert D. Alcohol septal ablation preceding transcatheter valve implantation to prevent left ventricular outflow tract obstruction. *EuroIntervention* 2018;**13**:2012–3.
5. Langhammer B, Huber C, Windecker S, Carrel T. Surgical antegrade transcatheter mitral valve implantation for symptomatic mitral valve disease and heavily calcified annulus. *Eur J Cardiothorac Surg* 2017;**51**:382–4.
6. El Sabbagh A, Eleid MF, Foley TA, Al-Hijji MA, Daly RC, Rihal CS *et al.* Direct transatrial implantation of balloon-expandable valve for mitral stenosis with severe annular calcifications: early experience and lessons learned. *Eur J Cardiothorac Surg* 2018;**53**:162–9.
7. Praz F, Khalique OK, Lee R, Veeragandham R, Russell H, Guerrero M *et al.* Transatrial implantation of a transcatheter heart valve for severe mitral annular calcification. *J Thorac Cardiovasc Surg* 2018;**156**:132–42.
8. Blanke P, Naoum C, Dvir D, Bapat V, Ong K, Muller D *et al.* Predicting LVOT obstruction in transcatheter mitral valve implantation: concept of the neo-LVOT. *JACC Cardiovasc Imaging* 2017;**10**:482–5.
9. Wang DD, Eng M, Greenbaum A, Myers E, Forbes M, Pantelic M *et al.* Predicting LVOT obstruction after TMVR. *JACC Cardiovasc Imaging* 2016;**9**:1349–52.
10. Nishimura RA, Otto CM, Bonow RO, Carabello BA, Erwin JP 3rd, Guyton RA *et al.* 2014 AHA/ACC Guideline for the management of patients with valvular heart disease: a report of the American College of Cardiology/American Heart Association Task Force on Practice Guidelines. *J Thorac Cardiovasc Surg* 2014;**148**:e1–e132.
11. Pressman GS, Movva R, Topilsky Y, Clavel MA, Saldanha JA, Watanabe N *et al.* Mitral annular dynamics in mitral annular calcification: a three-dimensional imaging study. *J Am Soc Echocardiogr* 2015;**28**:786–94.
12. Blanke P, Dvir D, Cheung A, Ye J, Levine RA, Precious B *et al.* A simplified D-shaped model of the mitral annulus to facilitate CT-based sizing before transcatheter mitral valve implantation. *J Cardiovasc Comput Tomogr* 2014;**8**:459–67.
13. Urena M, Himbert D, Brochet E, Carrasco JL, Iung B, Nataf P *et al.* Transseptal transcatheter mitral valve replacement using balloon-expandable transcatheter heart valves: a step-by-step approach. *JACC Cardiovasc Interv* 2017;**10**:1905–19.
14. Wang DD, Eng MH, Greenbaum AB, Myers E, Forbes M, Karabon P *et al.* Validating a prediction modeling tool for left ventricular outflow tract (LVOT) obstruction after transcatheter mitral valve replacement (TMVR). *Catheter Cardiovasc Interv* 2018;**92**:379–87.
15. Shivaraju A, Kodali S, Thilo C, Ott I, Schunkert H, von Scheidt W *et al.* Overexpansion of the SAPIEN 3 transcatheter heart valve: a feasibility study. *JACC Cardiovasc Interv* 2015;**8**:2041–3.
16. Yoon SH, Bleiziffer S, Latib A, Eschenbach L, Ancona M, Vincent F *et al.* Predictors of left ventricular outflow tract obstruction after transcatheter mitral valve replacement. *JACC Cardiovasc Interv* 2019;**12**:182–93.
17. Khan JM, Rogers T, Babaliaros VC, Fusari M, Greenbaum AB, Lederman RJ. Predicting left ventricular outflow tract obstruction despite anterior mitral leaflet resection: the "Skirt NeoLVOT". *JACC Cardiovasc Imaging* 2018;**11**:1356–9.